

Structure–Reactivity Relationships for Petroleum Asphaltenes

Murray R. Gray,* Martha L. Chacón-Patiño, and Ryan P. Rodgers

Cite This: *Energy Fuels* 2022, 36, 4370–4380

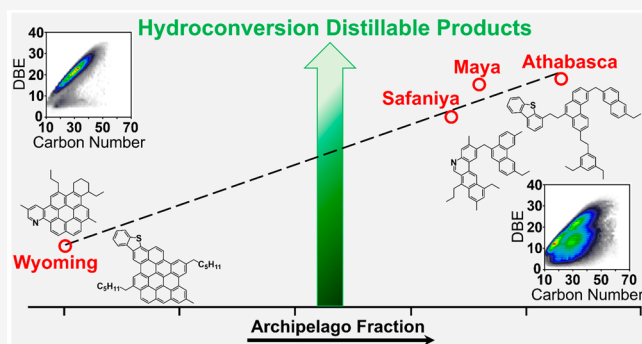
Read Online

ACCESS |

Metrics & More

Article Recommendations

ABSTRACT: The role of archipelago asphaltene structure in the reactions of petroleum asphaltenes was investigated by comparing yields of products from the conversion of archipelago-rich heavy oils and bitumen to the yields from a sample with predominant island-type structures. The archipelago content of the asphaltenes was positively correlated with the yield of liquid products boiling below 524 °C. The yield of coke solids increased with the fraction of island structures in the asphaltenes. Furthermore, catalytic hydroconversion of Athabasca bitumen gave a residual asphaltene fraction that was highly enriched in weakly aggregating components, on the basis of extrographic separation, and very low content of archipelago structures. High-resolution Fourier transform ion cyclotron resonance mass spectrometry (FT-ICR MS) analysis showed that the heteroatom polydispersity of the asphaltenes after conversion was dramatically reduced, and the range of double-bond equivalents and carbon number was close to the limiting boundary of planar polynuclear aromatic hydrocarbons (PAHs). The radical cations from the converted asphaltenes showed significant concentration of high-ring-number/known PAH structures. The results highlight the existence of a positive correlation between the amount of archipelago structural motifs in asphaltenes and the yield of products with a range of boiling points below 524 °C. Moreover, the data demonstrates that advanced hydroconversion methods can be used to obtain asphaltene fractions with decreased polydispersity in terms of heteroatom content, alkyl-substitution, and molecular structure, which could be eventually exploited for material science applications.



INTRODUCTION

Asphaltenes are the most complex fraction of petroleum that contain molecules of diverse heteroatomic functional groups, aromatic ring sizes, and attached alkyl chains. Evidence from thermal cracking of asphaltenes from heavy oils and bitumens has been consistent and unambiguously demonstrates the presence of reactive bridges between aromatic groups. The volatile products from thermal cracking at ~400–500 °C show high yields of one- to four-ring aromatics and heteroaromatics, along with one- to four-ring cycloalkanes, alkanes, and alkenes.^{1–5} The recent application of infrared multiphoton dissociation (IRMPD/gas-phase fragmentation) to ions trapped in ion cyclotron resonance mass spectrometers has confirmed the presence of both bridged aromatics, known as multicore or “archipelago” structures,⁶ and large aromatic ring groups with alkyl side chains, defined as single-core or “island” structures. Chacón-Patiño et al. recently reviewed the validation of these fragmentation studies.⁷ The observation of mixtures of island and archipelago structures was independently confirmed by high-energy collision-induced dissociation of narrow mass ranges of asphaltene ions.^{8,9} Recent work suggests that, in heavy crudes such as Athabasca, Safaniya, and Maya, archipelago structures dominate, but in at least one sample from a Wyoming wellbore deposit, island

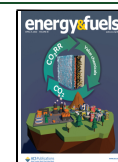
structures are dominant.^{7,10} Thermal cracking of Wyoming deposit asphaltenes in a thermogravimetric analyzer gave significant yields of cracked side chains and dealkylated aromatics, consistent with island structures and distinctly different from asphaltenes from heavy oils and bitumens.¹¹ These results suggest that the reaction properties of asphaltenes may depend strongly on the abundance of archipelago versus island structures.

When petroleum is processed in a refinery, distillation at atmospheric and vacuum conditions removes the more volatile components, producing a residue from vacuum distillation that is dominated by components boiling point over 524 °C. This vacuum residue contains C₇-asphaltenes at a concentration of up to 20 wt % and C₅-asphaltenes up to 30 wt % for crude oils such as Safaniya and Athabasca.¹² Three main types of technology can convert this vacuum residue to distillable products: coking, catalytic hydroconversion, and fluid catalytic

Received: February 19, 2022

Revised: March 26, 2022

Published: April 8, 2022



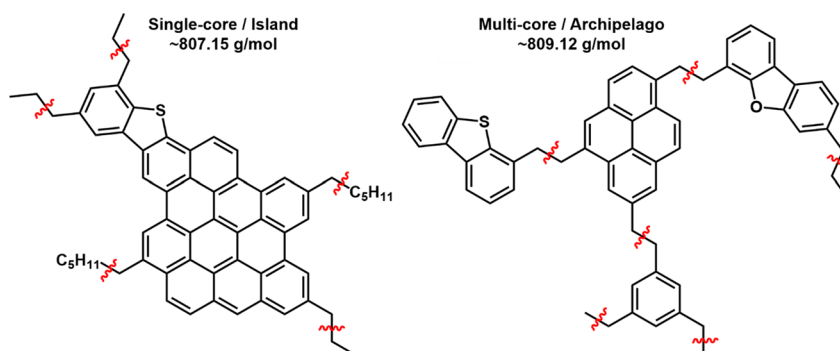


Figure 1. Products from cracking of single-core/island versus multicore/archipelago type asphaltene molecules. The red marks suggest the likely fragmentation sites in upgrading processes (e.g., thermal cracking, catalytic hydroconversion).

cracking. At low pressure and high temperatures over 480 °C, coking yields cracked fragments of the vacuum residue components and a solid highly aromatic product called “coke”. Catalytic hydroconversion uses high-pressure hydrogen and a catalyst to suppress the formation of coke, producing only liquid and gas products.¹³ Fluid catalytic cracking is suitable for lighter feeds that are mixtures of gas oil and vacuum residue with vanadium and nickel content below 30–40 ppm, restricting the concentration of asphaltenes.¹⁴ Insights from the analysis of asphaltene structure have the potential to link the performance of coking and hydroconversion processes in the refinery to the underlying chemistry of the feed. For instance, Ovalles et al.¹⁵ proposed that the reaction behavior of the asphaltene fraction alone is predictive of the entire vacuum residue fraction, even though the asphaltenes are only a fraction of the material. Understanding the relationship between the reactivity of the asphaltenes and their structural types can give insight into their behavior in refinery processes, as well as suggesting structure–reaction relationships for the broader vacuum residue fraction. This knowledge is central for the prediction of the chemistry of the products, which could guide novel applications such as the use of asphaltenes as precursor to carbon fibers.

The major reaction pathways for vacuum residues, including asphaltenes, during catalytic hydroconversion have been reported for many years.^{13,16–20} Reactions of model compounds of known molecular structures defined how each subunit of large molecules would behave, including aromatic, heteroatomic, cycloalkyl, and alkyl groups. Analytical data for the products of reaction was chained backward through the reaction pathways to construct consistent molecular representations for the starting vacuum residue. As more and more of the initial mass of vacuum residue is converted to volatile material, the remaining molecules are enriched in the least reactive structures and the rate of conversion with time declines.²¹ Similarly, the initial mass of asphaltenes is reduced by cracking reactions that remove attached aromatic, cycloalkyl, and alkyl groups, by catalytic hydrogenation that increases solubility in *n*-heptane and by hydrodesulfurization that increases solubility and reduces mass. The removal of side chains from *n*-heptane-soluble components will give some formation of new asphaltenes due to the reduced solubility of the remaining aromatic ring groups,²² but the net direction of reaction is a reduction in asphaltene content.

Thermal cracking of asphaltenes without a catalyst also removes attached aromatic, cycloalkyl, and alkyl groups.³ Without hydrogenation, the solubility of the asphaltenes

decreases with the time of reaction due to the loss of attached groups, formation of new molecules of low solubility from molecules in the maltene fraction,²² and by addition reactions within the asphaltene fraction.^{23–25} Eventually, the asphaltenes become insoluble in the liquid phase and solid coke forms very rapidly.²² The yield of coke has a complex dependence on the initial aromatic structures in the asphaltenes and vacuum residue, the rate of evaporation of molecular fragments from the liquid, and the rate of addition reactions.²⁶

Prior studies on asphaltene–reaction relationships examined reaction behavior as a function of H/C ratio,^{5,27} content of sulfur in sulfide groups,²⁸ and concentration of carbon and hydrogen types from nuclear magnetic resonance (NMR) spectroscopy.^{28,29} The rate of cracking of asphaltenes from different crude oils was most dependent on the concentration of sulfur in sulfides, one of the most reactive chemical groups in asphaltenes after carboxylic acids.^{28,29} Additional contributing factors were the concentration of alkyl groups attached to aromatic rings and the length of alkyl side chains.²⁹ Consistent with the importance of sulfides, the reactivity of whole vacuum residues was correlated with total sulfur content in a group of Venezuelan crude oils.³⁰ The yield of coke from thermal cracking of asphaltenes from different sources increased with the fraction of aromatic carbon as determined by ¹³C NMR spectroscopy, with coke yields determined by thermogravimetry⁵ or by cracking in batch microreactors.²⁸ Because molar H/C ratio is negatively correlated with the fraction of aromatic carbon, the yield of coke increased as molar H/C decreased for a series of asphaltenes from different crude oils.²⁷ However, none of these studies examined the role of archipelago versus island structural types in reaction kinetics or yields, except the comparison of the asphaltenes from the Wyoming deposit to Athabasca bitumen discussed above.¹¹

This paper examines two hypotheses regarding the reaction pathways of asphaltenes. The first is that a mixture dominated by archipelago structures will give more rapid conversion to volatile fragments than will a mixture based on island types. As illustrated in Figure 1 (right panel), the cracking of bridges between aromatic groups in an archipelago structure can give significant mass loss from each bond-breaking reaction, giving products with a range of boiling points below 524 °C. In contrast, an island-dominated mixture (structure to the left in Figure 1) will give smaller product fragments from side chains (i.e., gas and naphtha-range alkanes). The second hypothesis is that cracking of an archipelago-dominated asphaltene will give product asphaltenes that are dominated by island/single-core type structures due to the removal of attached aromatic and

Table 1. Properties of C₇-Asphaltenes from Different Sources Reacted by Catalytic Hydroconversion^{4,37} and Thermal Cracking^{28a}

source crude oil	molar H/C	sulfur, wt %	sulfide S by XPS ^b , wt %	aromaticity ^c , %	fraction of archipelago ^d , %	rate constant for thermal cracking at 430 °C ^e , min ⁻¹
Athabasca ⁴	1.11	8.0	1.5	50	86	0.15 ± 0.03
Maya ⁴	1.12	7.5	1.7	50	72	0.20 ± 0.09
Safaniya ⁴	1.12	7.9	1.1	51	67	0.17 ± 0.04
Wyoming Deposit ³⁷	1.06	1.8	na	na	<1	na

^ana – Not available. ^bWeight fraction of total sample as sulfur in sulfide groups, as determined by X-ray photoelectron spectroscopy using the method of Siskin et al.³⁸ ^cCarbon in aromatic rings as a percentage of total carbon, determined by ¹³C NMR spectrometry as described by Sheremata et al.³⁹ ^dFraction of archipelago estimated from fragmentation spectra of precursor ions at *m/z* 453–457 for the extrography fractions, as illustrated in Figure 8, added in proportion to the yield of each fraction^{10,35,36} ^eApparent first order rate constant for thermal cracking in 1-methylnaphthalene, from fitting of yields from 10–60 min of reaction at 430 °C to the kinetic model of Wiehe²²

cyclo-alkyl groups. Cracking of the alkyl bridges in the structure to the right in Figure 1 yields single core molecules. Depending on the size of the aromatic core (ring number), the remaining cores can be alkane insoluble/toluene soluble (asphaltenes). The first hypothesis is examined by comparing the structure with available data on reactivity using recent data on the abundance of archipelago structures in asphaltenes from different sources. The second hypothesis is tested using data on Athabasca asphaltenes before and after conversion by catalytic hydroconversion.

EXPERIMENTAL METHODS

Materials. High-performance liquid chromatography (HPLC)-grade solvents were used as received: acetone, *n*-pentane (C₅), *n*-heptane (C₇), toluene (Tol), methanol (MeOH), and dichloromethane (DCM) were purchased from J.T. Baker. HPLC-grade tetrahydrofuran (THF) with no solvent stabilizer was purchased from Alfa Aesar. Chromatographic-grade silica gel (100–200 mesh, type 60 Å, Fisher Scientific) was used for extrography separation, Whatman filter papers grade 42 were employed for asphaltene recovery, and high-purity glass microfiber thimbles were used for Soxhlet extraction (Whatman, GE Healthcare, Little Chalfont, U.K.).

Precipitation of Asphaltenes. Asphaltenes were precipitated from Wyoming deposit and Athabasca bitumen oils, before (untreated) and after hydroconversion, using a slightly modified ASTM method, as described elsewhere.³¹ Crude oils (~10 g) were sonicated at 60 °C, meanwhile 400 mL of *n*-heptane was added dropwise. The mixture was allowed to stand overnight, and precipitated solids (unclean asphaltenes) were separated from maltenes by filtration and extracted with C₇ in a Soxhlet apparatus for 168 h. C₇-asphaltenes were recovered by dissolution in hot toluene (~98 °C), which was evaporated under nitrogen to yield solid C₇-asphaltenes. Subsequently, C₇-asphaltenes were cleaned by four cycles of crushing-extraction, as previously reported, to decrease the content of occluded maltenes.³¹

Extrography Fractionation Method. Asphaltenes were dissolved in DCM (200 µg/mL) and mixed with silica gel (10 mg of asphaltenes/1 g of SiO₂). The mixture was dried under nitrogen and subsequently placed into glass microfiber thimbles in a Soxhlet apparatus. Asphaltene fractions were extracted using acetone, Hep/Tol (1/1), and Tol/THF/MeOH (5/5/1). Extraction with each of the solvents lasted 24 h and was performed under a N₂ atmosphere to prevent oxidation. Fractions were dried under nitrogen, weighted, and stored in the dark for subsequent mass spectrometry analysis via positive-ion atmospheric pressure photoionization (+APPI) coupled to Fourier transform ion cyclotron resonance mass spectrometry (FT-ICR MS).

(+) APPI FT-ICR MS Analysis. Asphaltenes and extrography fractions were dissolved in toluene (50 µg/mL) and directly infused at 50 µL/min into a Thermo-Fisher Ion Max APPI source (Thermo-Fisher Scientific, Inc., San Jose, CA) operated with a vaporizer temperature of 340 °C and supplied with N₂ sheath gas (50 psi) and

N₂ auxiliary gas (16 mL/min). Gas-phase neutrals were photoionized by a 10 eV (120 nm) ultraviolet krypton lamp. Samples were analyzed with a custom-built 21 T FT-ICR mass spectrometer, where the application for complex mixtures is described elsewhere.³² Approximately ~150 (APPI) time-domain acquisitions were coadded, Hanning-apodized, and zero-filled once before Fourier transform and magnitude calculation. Spectra were internally calibrated using extended homologous alkylation series of high/medium relative abundance before peak detection [$>6\sigma$ baseline root-mean-square (RMS) noise] and automated elemental composition assignment. PetroOrg Software provided molecular formula assignments and data visualization via plots of double bond equivalents (DBE = number of rings plus double bonds to carbon, also referred as aromaticity in petroleomics³³) versus carbon number.

Stored Waveform Inverse Fourier Transform (SWIFT) Excitation and Infrared Multiphoton Dissociation (IRMPD) of Asphaltenes. Mass segments of 4 Da width were isolated via a quadrupole ion guide before external ion accumulation (accumulation period = 2–10 s) and subsequently transferred to the 9.4 T FT-ICR cell for selective isolation of high DBE precursor ions, mass measurement, and infrared multiphoton dissociation (IRMPD). The method was described in detail by Niles et al.³⁴ IRMPD ($\lambda = 10.6 \mu\text{m}$, 40 W, 50–1000 ms irradiation, Synrad CO₂ laser, Mukilteo, WA) provided gas-phase dissociation of the isolated precursor ions inside the FT-ICR cell (pressure $<10^{-10}$ Torr). PetroOrg Software provided molecular formula assignment for precursor ions and the fragment ions.

RESULTS AND DISCUSSION

Hydroconversion of Asphaltenes from Different Sources. Four asphaltene samples with a wide range of archipelago content that were subjected to catalytic hydroconversion in a batch reactor at 450 °C. The conditions were selected to give maximal yield of liquid products with minimal yield of solid coke.⁴ The addition of an iron catalyst suppressed coke formation but gave low activity for sulfur and nitrogen removal, and tetralin helped to maintain soluble products.

The data of Table 1 present some chemical features (e.g., bulk H/C ratios) of the reacted asphaltenes. The yield of coke was significantly higher for C₇-asphaltenes from the Wyoming deposit sample than from the heavy crude oils, and the yield of distillable products for Wyoming deposit was less than one-half the yield from the heavy oils, as illustrated in Figure 2, which presents the yield of coke (black marker) and distillable products (white) as a function of an approximated archipelago content. The fraction of archipelago was estimated from the fragmentation spectra of precursor ions. Here, we focused on ions containing C, H, and one S atom (S₁ class) with *m/z* values between 450 and 455.

The selection of higher MW ranges results in increased proportions of multicore/archipelagos in all asphaltene

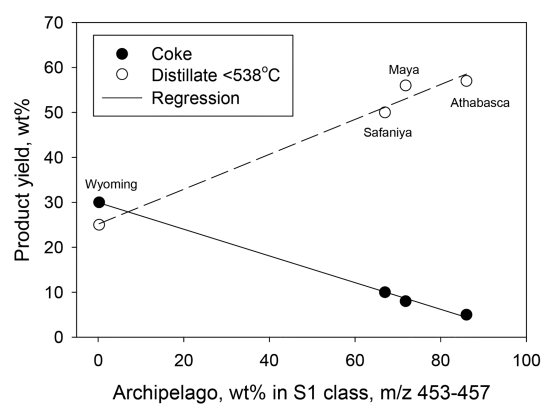


Figure 2. Product yield from catalytic hydroconversion as a function of archipelago structure.^{4,37} Reaction was in a batch reactor at 450 °C and 10 MPa hydrogen pressure for 3 h with 2.5:1 tetralin and 2% iron-based catalyst. The lines in the figure are from linear regression.

samples studied by IRMPD⁷ and other dissociation methods,^{8,9} and thus, interrogation of higher m/z species maintains the observed relative trends. When precursor ions belong to compound classes with a higher heteroatom content, the complexity of the data analysis is dramatically increased, as heteroatoms might be present in different cores, and after fragmentation, precursor ions belonging to one compound class can yield fragments of several classes. Previously, it was reported that precursor ions that are enriched in polyheteroatomic species (e.g., N_1O_2 , S_2 , S_3 , $N_1O_1S_1$) tend to produce IRMPD fragments with increased relative abundances of hydrocarbons and monoheteroatomic classes (i.e., S_1 , N_1 , O_1).³⁵ This result is due to the fragmentation of polyheteroatomic archipelago precursor ions, with heteroatoms present in different cores, which reveal a tendency to produce a lower carbon number and lower DBE fragment ions with fewer heteroatoms.

Details for the calculation of the relative content of island vs archipelago are reported elsewhere and rely on APPI FT-ICR MS and IRMPD characterization of asphaltene samples.³⁶ In short, the mass spectra for the selected precursor ions provide an island/archipelago boundary, defined as the abundance weighted average of DBE values for the precursor ions minus the weighted standard deviation. Fragmentation mass spectra provide the relative abundance of fragments with an island or archipelago structure: fragment ions below the island/archipelago boundary, with much lower DBE values than those of the precursor ions, are derived from archipelago species because substantial loss of DBE is only possible when multicore structures are present.³⁶ In this work, the fraction of archipelago was reported for S_1 compounds; the reason for selecting this compound class is based on reports that suggest that a low sulfur content in heavy feedstocks (i.e., sulfide groups) has been noted for samples with low conversion yields.^{29,30}

The data of Figure 2 suggest a high correlation between conversion yields at constant hydroconversion conditions and the fraction of archipelago S_1 structures in the starting sample. Although the data are persuasive, the sample set is limited and samples in the range 1–60% archipelago fraction are lacking to confirm the linear correlation. The low concentration of sulfur in the Wyoming deposit (Table 1) suggests a much lower concentration of reactive sulfide groups, given one-quarter as

much total sulfur and assuming a fraction of sulfide sulfur (14–22%)⁴ comparable to the other samples.

Thermal Cracking and Coking of Asphaltenes from Different Sources. The yield of coke from thermal cracking of asphaltenes and vacuum residues can be compared using thermogravimetric analysis (TGA) in nitrogen or argon. The asphaltene samples listed in Table 1 were reacted to an end temperature of 500 °C in an inert atmosphere. Figure 3

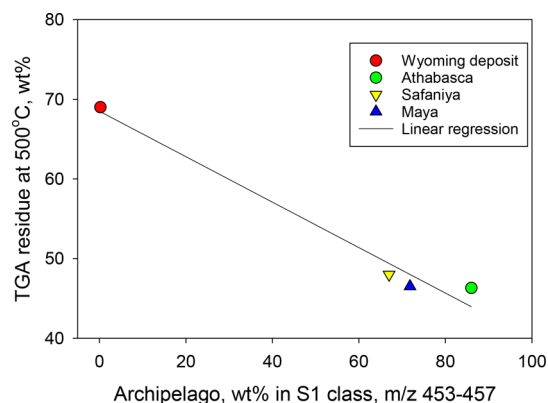


Figure 3. Yield of solid residue from reaction in a thermogravimetric analyzer at 500 °C end temperature as a function of archipelago content.^{4,37}

presents the amount of residue (solid coke) upon TGA versus the estimated archipelago content. The yield of solid coke residue was substantially higher from the Wyoming deposit (~68 wt %), suggesting that the much lower archipelago content gave less evolution of cracked products to the vapor phase. The yield of coke from asphaltenes also correlates with the fraction of aromatic carbon⁵ and gives a negative correlation with H/C ratio.²⁷ The Wyoming sample features the lowest H/C ratio of the samples listed in Table 1, but the value of 1.06 gives an estimated aromatic carbon fraction of 53% from the data of Calemma and Rausa,⁵ very similar to the other samples listed in Table 1. Consequently, the difference in aromatic carbon content cannot explain the difference in reaction yield. As in the data from catalytic hydroconversion, the low content of reactive sulfur groups in the Wyoming sample could be a factor contributing to the higher coke yield.

Although the idea of a linear correlation between archipelago content for S_1 species and coke yield from thermal cracking is appealing, the data set in Figure 3 is highly limited in terms of the number of samples and the distribution over the range of archipelago content to allow a general conclusion. Validation of the proposed linear correlation should include asphaltene samples with estimated archipelago contents between 5 and 60 wt % and TGA residue of ~50–65 wt %.

Additionally, Rahmani et al.²⁸ compared the thermal cracking rates of Athabasca, Maya, and Safaniya C_7 -asphaltenes in 1-methylnaphthalene solvent. The first order rate constants fell in a narrow range from 0.15 to 0.20 min^{-1} with no statistically significant differences (Table 1), consistent with the relatively narrow range of archipelago fraction from 67 to 86%. Thus, the reported data on thermal cracking is consistent with the extrography/MS determination of archipelago content in the studied samples.

Thermal Cracking of Vacuum Residues from Different Sources. Following the continuum concept of Boduszynski,^{33,40} we expect similar molecular features in the heavy

fractions of crude oil as the C₇-asphaltenes, so that differences in the structure of the asphaltenes between different crude oils may predict the behavior of the whole crude.¹⁵ Such a relationship is most likely for reactions like thermal cracking where the heavy fractions are dominant. Although many heavy crude oils processed in refineries fall in a narrow band of reactivity, Rubiales crude oil from Colombia reveals an anomalously low conversion under thermal cracking conditions.²⁹ Under conditions where Athabasca vacuum residue gave 38% conversion, Rubiales gave almost no detectable conversion (Table 2). The Wyoming deposit, which has an

Table 2. Properties and Reactivity of Vacuum Residues from Different Sources Reacted by Thermal Cracking²⁹ with Archipelago Fraction of C₇-Asphaltenes

properties and conversion	Athabasca	Rubiales
sulfur in crude oil, wt %	4.9	1.3 ⁴¹
aromatic carbon in crude oil, %	36	31
fraction of archipelago in C ₇ -asphaltene fraction, % ^a	86	50
conversion of vacuum residue, wt % ^b	38.4	0.8
coke yield, wt % ^b	1.7	3.3

^aFraction of archipelago estimated from fragmentation spectra of S₁ precursor ions at *m/z* 453–457 for the extrography fractions, as illustrated in Figure 8, added in proportion to the yield of each fraction.^{10,35,36} ^bReaction in a batch reactor at 405 °C for 30 min after reaching final temperature

insignificant content of archipelago structures, still gave one-half the yield of cracked products as Athabasca (Figure 2), not less than one-tenth as in the case of Rubiales. Thus, factors other than the fraction of archipelagos must contribute to the unusual behavior of Rubiales. The low sulfur content may play a role, giving such a low content of reactive sulfide sulfur.^{28,30} Other features that could play a role include the nitrogen, oxygen, and metals components, the low reactivity of the resins in the vacuum residue, or an unusual tendency to give addition products. The source kerogen and geological maturity may play an important role in determining many of these features of the asphaltene fraction.

Asphaltene Molecular Structures Before and After Catalytic Hydroconversion. In order to test the hypothesis that an archipelago-rich bitumen could give product asphaltenes after catalytic hydroconversion that were rich in island structures, we analyzed a sample of Athabasca C₇-asphaltenes after 77% conversion of the vacuum residue fraction.⁴² Asphaltenes were precipitated from the untreated bitumen and the hydroconverted products and subjected to extrography fractionation. Extrographic separation gave three subfractions, acetone, Hep/Tol, and Tol/THF/MeOH, which were analyzed by FT-ICR MS, and gas-phase fragmentation of selected precursor ions was performed via IRMPD. Ultrahigh-resolution mass spectrometry, or FT-ICR MS, works as a molecular-level elemental analyzer and provides the molecular formula or elemental composition for tens-of-thousands of ions. The ultrahigh mass accuracy enables access to the molecular composition of ultracomplex mixtures such as heavy petroleum and dissolved organic matter. However, it should be noted that the analyses are limited by the ability of ions sources (e.g., APPI) to indiscriminately volatilize and ionize the compounds within the samples.⁷ Additionally, for the samples discussed herein, bulk elemental analysis suggests that cracking reactions removed hydrogen-rich attached groups, increasing

the aromatic carbon fraction from ca. 50% in the feed to ca. 70% in the product (estimated from H/C ratios using the data of Calemma and Rausa⁵). Extensive catalytic hydrodesulfurization reduced the sulfur content by half, but hydrodenitrogenation was much less effective, giving significant accumulation of unreactive nitrogen compounds in the product (Table 3).

Table 3. Properties of Athabasca C₇-Asphaltenes before and after Catalytic Hydroconversion⁴²

source crude oil	H/C	S/C	N/C	fraction of archipelago, % ^a
Athabasca	1.130	0.030	0.010	86 ¹⁰
hydroconverted Athabasca ^b	0.786	0.014	0.018	4

^aFraction of archipelago estimated from fragmentation spectra of precursor ions at *m/z* 453–457 for the extrography fractions, as illustrated in Figure 8, added in proportion to the yield of each fraction.^{10,35,36} ^bSample was separated from an Athabasca residue fraction subjected to catalytic hydroconversion to achieve 77% conversion of the vacuum residue fraction.

The gravimetric results for the extrography separation suggest that the combination of cracking and catalytic reactions had a dramatic impact on the distribution of the extrography fractions. Figure 4 presents the gravimetric yields for the extrographic fractionation of several asphaltene samples. In the ternary diagram, each coordinate axis represents one extrography fraction: acetone, Hep/Tol, and Tol/THF/MeOH plus unrecovered material. It has been suggested that the sample's clustering tendency in the ternary plot is consistent with their compositional differences (island vs archipelago content) and their tendency to produce coke in upgrading processes. For example, the acetone fraction is abundant for Wyoming deposit asphaltenes (~37 wt %, 69% of coke production), whereas Athabasca bitumen asphaltenes reveal abundant Tol/THF/MeOH (~52 wt %, 46.3% coke by TGA) and Maya asphaltenes give abundant Hep/Tol (~65 wt %, 46.5% coke by TGA) fractions; these samples are located in different parts of the plot. Figure 4 highlights the dramatic change in composition for the hydroconverted Athabasca bitumen asphaltenes: with an acetone fraction content of >80%, the asphaltenes from the hydroconverted bitumen shift to the lower-right side of the ternary plot. It is critical to highlight that previous reports show that acetone fractions from geologically diverse asphaltenes contain abundant island motifs, which are depleted in polyheteroatomic compounds (e.g., oxygen rich species) and present much weaker deposition/aggregation trends compared to whole asphaltenes and Tol/THF/MeOH fractions.^{43,44} Thus, the increased content of the least aggregating (island-rich) acetone fraction for the hydroconverted sample is consistent with a significant reduction in compound classes containing oxygen atoms (Figure 5, compound class distribution derived from FT-ICR MS analysis). There is a remarkable decrease for the Tol/THF/MeOH fraction: from ~52 wt % in the unreacted Athabasca bitumen asphaltenes to ~8 wt % for the hydroconverted sample. This highly "polar" extrography fraction has been shown to contribute to disproportionately high aggregation. Its decreased content in the hydroconverted sample is consistent with the low degree of aggregation as determined by vapor-pressure osmometry in toluene solutions over a range of sample concentration.⁴²

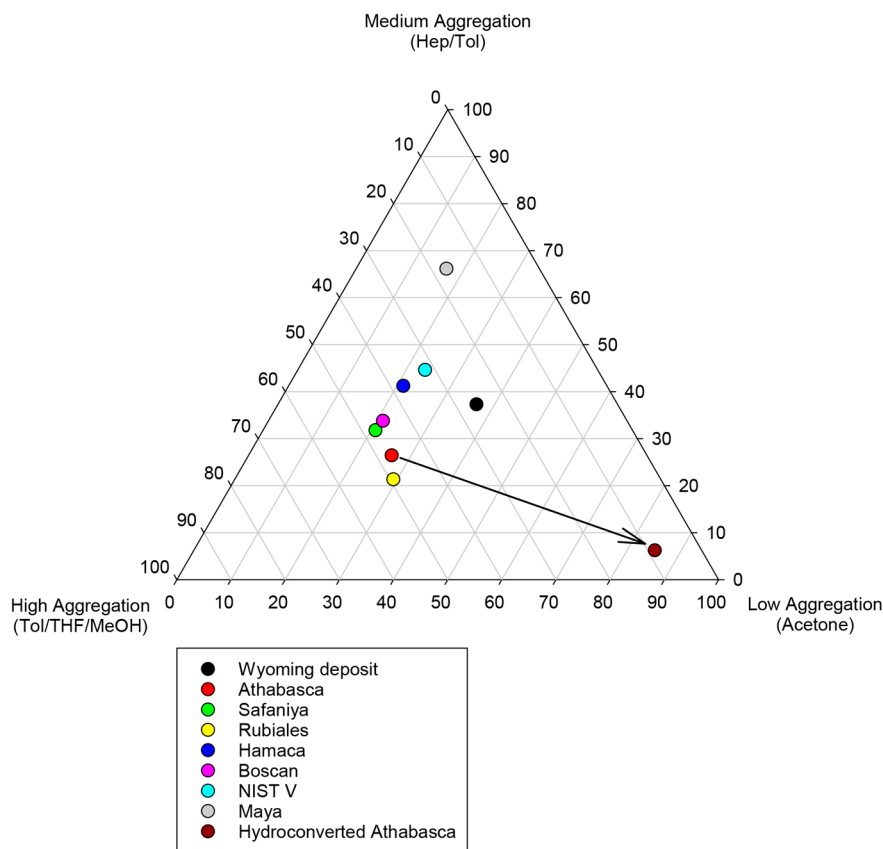
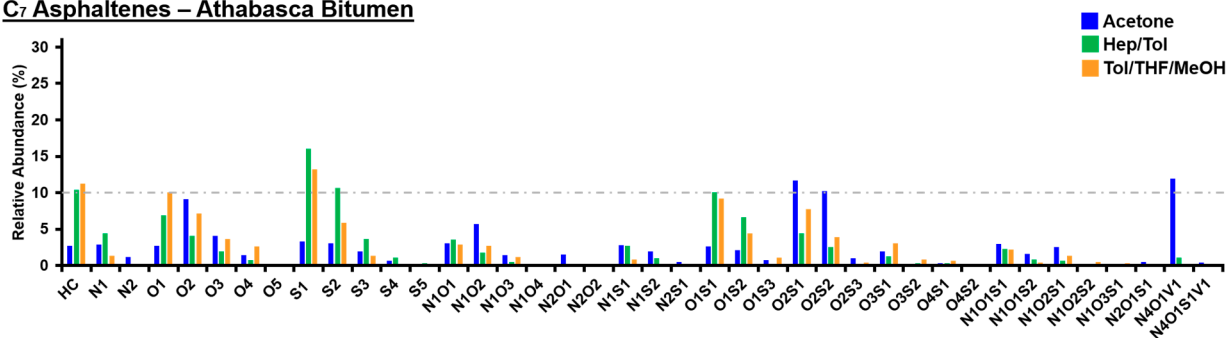


Figure 4. Concentration of extrographic subfractions as weight% by extraction with acetone, heptane + toluene (Hep/Tol), and toluene + tetrahydrofuran + methanol (Tol/THF/MeOH). Data for unreacted samples are from Chacón-Patiño et al.⁷

C₇ Asphaltenes – Athabasca Bitumen



C₇ Asphaltenes – Hydroconverted Athabasca Bitumen

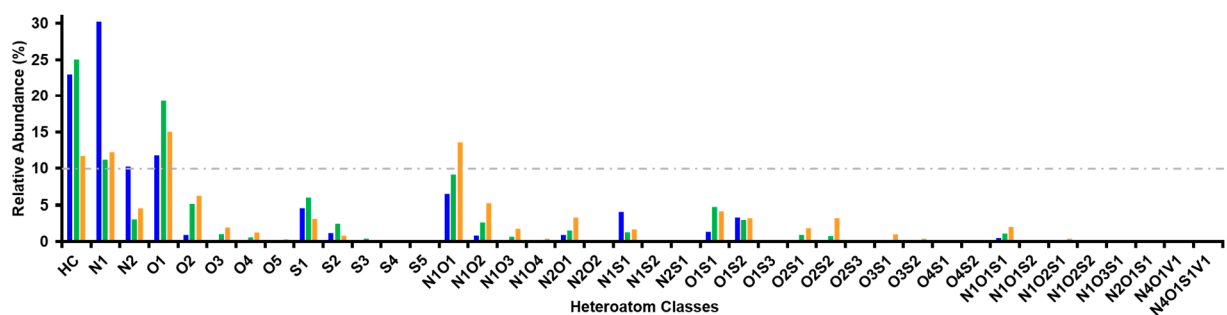


Figure 5. Heteroatom class distribution from Athabasca C₇-asphaltenes before (upper panel) and after (lower panel) catalytic hydroconversion.

Molecular Characterization of Asphaltene Samples:
 (+) APPI FT-ICR MS and IRMPD. Molecular formulas accessed via FT-ICR MS are classified in compound classes. For example, the HC class comprises species with only C and

H atoms. Compounds with C, H, and one S atom belong to the S₁ class. Vanadyl porphyrins, whose tetrapyrrole core contains four N atoms and a vanadyl group (V=O), are denoted as the N₄O₁V₁ class. Figure 5 presents the compound

class distribution for the extrography fractions from C_7 -asphaltenes derived from untreated (upper panel) and hydroconverted (lower panel) Athabasca bitumen. The results demonstrate that hydroconverted asphaltenes are less polydisperse in terms of heteroatom content: after hydroconversion, there is an increase (~ 2 – 10 -fold) in the content of hydrocarbons with no heteroatoms (HC class) and monoheteroatomic classes (N_1 , O_1), with concurrent significant decrease, or no detection, for polyheteroatomic classes such as N_2 , S_2 , S_3 , S_4 , O_1S_2 , O_2S_2 , $N_1O_1S_2$, and vanadyl porphyrins $N_4O_1V_1$.

Molecular formulas accessed via FT-ICR MS can be visualized in isoabundance contoured plots of double bond equivalents (DBE or “aromaticity”) versus carbon number; in those plots, the color scale represents the relative abundance. A higher DBE indicates that the detected ions have more rings and double bonds (higher aromaticity). At a constant DBE, a higher carbon number denotes increased content of CH_2 units (more alkylation). Figure 6 presents the combined DBE vs

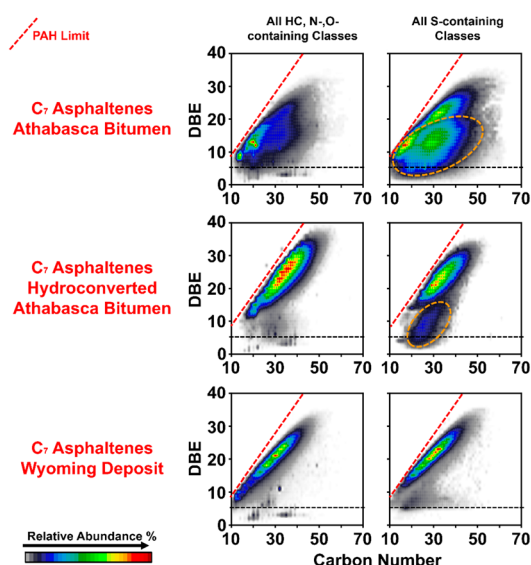


Figure 6. Combined isoabundance color-contoured plots of DBE vs carbon number for HC- and N-/O-containing species (plots to the left) and S-containing compounds (plots to the right) for all extrography fractions from raw Athabasca C_7 -asphaltenes, hydroconverted Athabasca C_7 -asphaltenes, and Wyoming deposit C_7 -asphaltenes.

carbon number plots for all detected compound classes (except vanadyl porphyrins) for all the extrography fractions derived from C_7 -asphaltenes from Athabasca bitumen (upper row), hydroconverted Athabasca bitumen (middle row), and Wyoming deposit (lower row). Classes have been grouped into HC + N-/O-containing species (plots to the left) and all S-containing compounds (plots to the right). The results indicate that S-containing classes have a multimodal compositional range: there are compounds with low carbon number/high DBE and species with much lower aromaticity (circled in orange). This feature is more prominent for untreated Athabasca bitumen asphaltenes, for which the abundant detection of low-DBE/high-carbon number S-containing compounds (DBE < 5, $C\# > 35$) suggests the presence of reactive S functionalities, e.g., sulfides/sulfoxides, as previously reported by Ballard et al.⁶ FT-ICR MS results indicate that

these compositions are practically absent in the Wyoming deposit asphaltenes (Figure 6, bottom, right). Interestingly, low-DBE S-containing compounds with $C\# < 35$, are detected for the hydroconverted sample, but with a much lower relative abundance/carbon number(s) than the untreated asphaltenes. Furthermore, for Athabasca bitumen, the asphaltene components that remained after hydroconversion reveal higher double-bond equivalents (DBE) than the feed and had DBE and carbon number values that were much closer to the polyaromatic hydrocarbon (PAH) limit (Figure 6, red dotted line). The PAH limit is a compositional boundary for fossil fuel compounds that dictates the highest possible DBE value, at a given carbon number, for planar/near planar petroleum molecules (pericondensed PAHs). DBE values above this limit correspond to nonplanar species (fullerene-like compounds).⁴⁵ Table 4 includes the abundance-weighted average

Table 4. Abundance-Weighted Average DBE Values and H/C Ratios Derived from the APPI FT-ICR MS Characterization of the Extrography Fractions

sample	DBE	H/C
untreated Athabasca bitumen asphaltenes	15.2	1.21
hydroconverted Athabasca bitumen asphaltenes	21.0	0.78
Wyoming Deposit asphaltenes	21.3	0.84

DBE values and H/C ratios derived from the APPI FT-ICR MS characterization of the extrography fractions for the three samples, calculated as previously reported.⁷ The results prove that hydroconversion yields asphaltene species with a much higher aromaticity (DBE values), consistent with prior analysis of asphaltenes after hydroconversion.^{8,20,46} The hydroconverted asphaltenes reveal an average DBE and H/C ratio comparable to Wyoming deposit asphaltenes. However, as further discussed below, both samples reveal marked molecular-level differences uniquely detected by FT-ICR MS.

A zoom-inset to the compositional range for selected classes for the acetone fraction for the three asphaltene samples (radical cations $[M\cdot+]$ for HC and N_1 classes), shown in Figure 7, suggests that the distribution of components for asphaltenes derived from the hydroconverted bitumen was much closer to the PAH limit than the Wyoming deposit sample. Importantly, Wyoming asphaltenes are rich in island structures.¹⁰ Figure 7, right panel, highlights the presence of abundant known PAHs in the hydroconverted asphaltenes.^{47,48} Understanding the effect of upgrading (i.e., thermal cracking and hydroconversion) on asphaltene structure is central to optimal use of petroleum residues for production of carbon fibers. Critical properties such as pitch spinnability should be highly dependent on sample’s molecular structure and the presence of alkyl-depleted PAHs,⁴⁹ which are highly abundant in heavy fractions from upgraded petroleum residues.

Gas-Phase Fragmentation via IRPMD. The gravimetric results for the extrography fractionation suggest that hydroconverted Athabasca bitumen asphaltenes contain abundant island structures that result in weak aggregation in solution, which is characteristic for the acetone extracted species. Furthermore, the gas-phase fragmentation of the extrographic fractions of hydroconverted Athabasca confirmed the hypothesis that catalytic hydroconversion would convert an archipelago-rich mixture to an island-rich mixture. Figure 8 presents the compositional range for the extrography fractions for C_7 -asphaltenes from untreated and hydroconverted

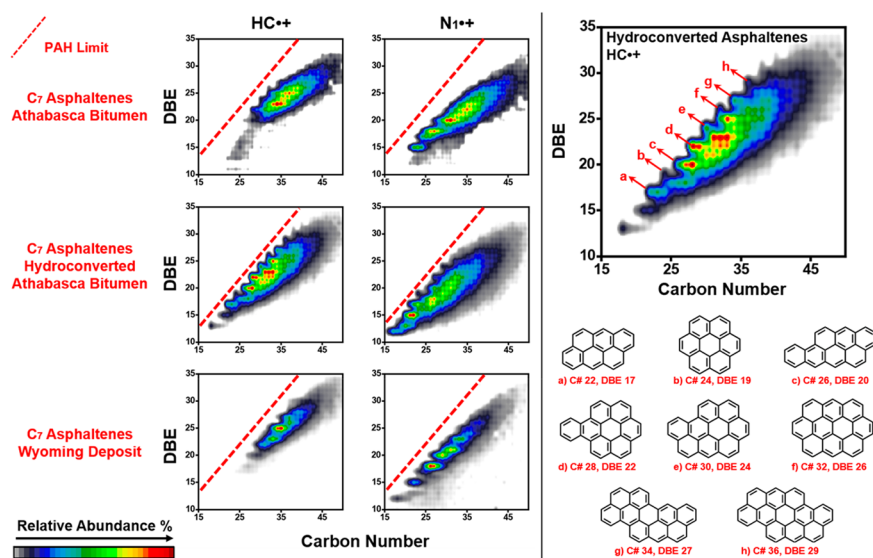


Figure 7. Left: zoom-inset on the compositional range of HC and N_1 radical cations for the acetone fractions for C_7 -asphaltenes from raw/hydroconverted Athabasca bitumen and Wyoming deposit. Right: abundant polycyclic aromatic hydrocarbons (PAHs) found in the HC^{++} for the acetone fraction for the hydroconverted asphaltenes.

Athabasca bitumen (all compound classes combined except vanadyl porphyrins) and the corresponding fragmentation mass spectra for precursor ions with $m/z \sim 450$. As previously reported, petroleum precursor ions (red asterisks in the mass spectra of Figure 8) reveal two major fragmentation pathways: dealkylation, highlighted by the green arrow in the fragmentation mass spectra, and “bridge” dissociation products, highlighted by the orange dashed line. Molecular formula calculation for the fragments from dealkylation demonstrates that the ions keep the same DBE range than precursors and predominantly lose carbon number due to the fragmentation of alkyl side chains. This behavior is consistent with single-core motifs (island, Figure 1, left panel). The fragments from bridge dissociation are diagnostic for multicore structures (archipelago, Figure 1, right panel) because they present a lower carbon number and lower DBE values than the precursor ions. The low molecular weight distribution highlighted between $m/z \sim 120$ and 300 for the Tol/THF/MeOH fraction from untreated Athabasca bitumen asphaltenes mainly consists of 1–5-ring aromatics with various degrees of alkyl substitution. The detection of these species from the gas-phase fragmentation of high-DBE asphaltene precursor ions (DBE > 19) is consistent with the presence of archipelago structures.

Furthermore, Figure 8, lower panel, suggests that hydroconversion cracked bridges between aromatic and cycloalkyl groups, which decreased the archipelago content in the acetone and Hep/Tol fractions to undetectable levels. Only the Tol/THF/MeOH fraction retained detectable archipelago structures. Additionally, it is important to point out the remarkable low abundance of fragments, relative to precursor ions, for the hydroconverted asphaltenes. Under the same experimental conditions, untreated Athabasca bitumen C_7 -asphaltenes produced fragment ions with much higher relative abundance. Thus, untreated asphaltenes reveal a higher reactivity in IRMPD, which could be due to the higher content of longer alkyl-side chains and oxygen-containing functionalities, such as carboxylic acids and sulfoxides, well-known for their efficient absorption of infrared light.

The mass-weighted sum of the archipelago content of the fractions in Figure 8 showed a decrease from $\sim 86\%$ in the feed to only $\sim 4\%$ (Table 3), which confirms the hypothesis. The comparison between Athabasca, hydroconverted Athabasca, and the Wyoming deposit samples demonstrates that the combination of extrographic separation, FT-ICR MS, and IRMPD enables the discrimination of samples rich in archipelago structures from those rich in island structures.

The hydroconverted sample was from medium conversion conditions, giving 77% conversion of vacuum residue. At higher conversion levels with supported-metal catalysts, the precipitation of the asphaltenes to form “sludge” can be a significant issue,^{13,14,50} which can be circumvented by using dispersed metal catalysts.⁵¹ The analytical methods presented in this paper could be valuable in understanding the molecular basis for asphaltene aggregation and precipitation at higher levels of conversion.

The comparisons of structure and reactivity in this paper have two limitations. The first, as discussed above, is the limited sample set of asphaltene samples for which there are both structural information and reaction data. While heavy oils are well-represented, analysis of trends is hindered by the large gap in archipelago and sulfur content between Athabasca, Safaniya, and Maya at one extreme and Wyoming deposit at the other. The second limitation is the metric for the archipelago content of each asphaltene sample, using IRMPD fragmentation of ions in a narrow band of m/z followed by integration of the S_1 fragment yields to estimate archipelago and island structural types. The parent ions in this analysis may also contain oxygen and nitrogen atoms, and fragments that do not contain sulfur are not included for the archipelago estimation presented herein. For sulfur-rich samples, these limitations are unlikely to bias the results, but samples with very low sulfur content may not give representative data.

Regardless of the limitations, the presented results demonstrate the potential of chemical separations, FT-ICR MS, and IRMPD to understand and predict petroleum processability in catalytic hydroconversion and thermal cracking. Furthermore, the results highlight the application of

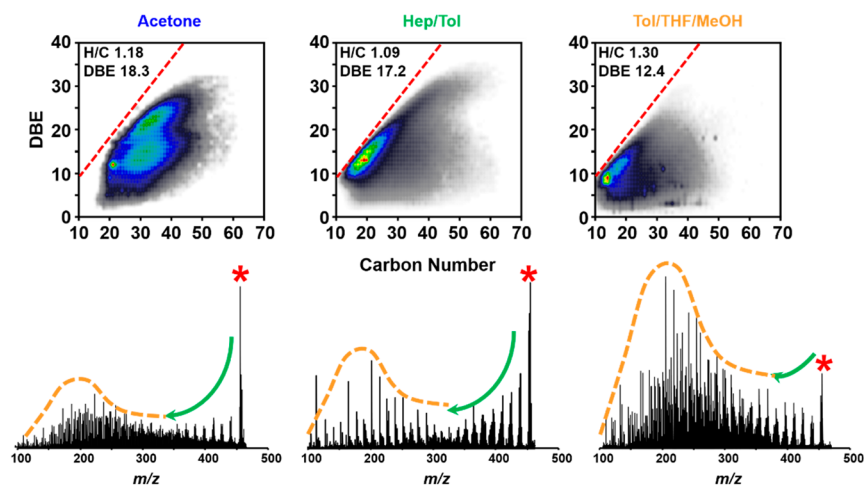
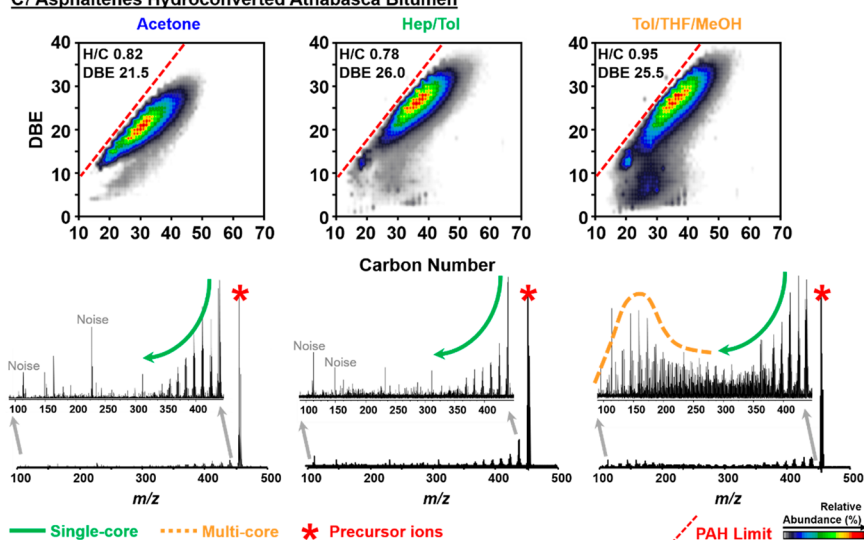
C₇ Asphaltenes Athabasca BitumenC₇ Asphaltenes Hydroconverted Athabasca Bitumen

Figure 8. Color-contoured isoabundance plots of DBE versus carbon number for all compound classes (except vanadyl porphyrins) and fragmentation spectra of precursor ions with m/z 453–457 for the extrography fractions derived from Athabasca Bitumen C₇-asphaltenes before (top panel) and after (bottom panel) catalytic hydroconversion. Abundance weighted H/C ratios and DBEs are included and demonstrate the much higher aromaticity of the asphaltenes obtained from the hydroconverted bitumen.

upgrading processes to produce petroleum heavy fractions with decreased polydispersity in terms of heteroatom content, alkyl-chain content, and structural diversity. C₇-asphaltenes from the hydroconverted Athabasca bitumen reveal a disproportionately high concentration of island/single-core motifs and high ring-number PAHs, which could be explored for material-science applications (e.g., carbon fibers).

CONCLUSIONS

The yields of products from C₇-asphaltene fractions of Athabasca, Maya, Safaniya, and Wyoming deposit under catalytic hydroconversion and thermal cracking conditions were highly correlated with the abundance of archipelago S₁ compounds of asphaltenes. S-containing compounds were selected for correlations because the abundant presence of reactive S species, e.g., sulfides, has been reported for vacuum residues with high conversion yields. Archipelago-rich asphaltenes gave much higher yields of liquid products, and lower yields of coke, than the island-rich Wyoming deposit

sample. At a high extent of conversion, the archipelago-rich Athabasca asphaltenes were almost completely converted to island structures, consistent with the removal of attached groups by thermal cracking, fragmentation of bridges between aromatic cores, and removal of heteroatoms. The remnant asphaltenes after conversion dramatically reduced the polydispersity of heteroatom classes and were highly enriched in identified polynuclear aromatic hydrocarbons with a low extent of alkyl substituents. Validations of these correlations require the characterization of samples with estimated archipelago contents between 5 and 60 wt % and TGA residue of ~50–65 wt %.

AUTHOR INFORMATION

Corresponding Author

Murray R. Gray – Department of Chemical and Materials Engineering, University of Alberta, Edmonton, AB T6G 1H9, Canada; orcid.org/0000-0003-2431-7312; Email: murray.gray@ualberta.ca

Authors

Martha L. Chacón-Patiño – Ion Cyclotron Resonance Program, National High Magnetic Field Laboratory, Florida State University, Tallahassee, Florida 32310, United States; International Joint Laboratory iC2MC: Complex Matrices Molecular Characterization, Total Research & Technology, Gonfreville 76700 Harfleur, France; orcid.org/0000-0002-7273-5343

Ryan P. Rodgers – Ion Cyclotron Resonance Program, National High Magnetic Field Laboratory, Florida State University, Tallahassee, Florida 32310, United States; International Joint Laboratory iC2MC: Complex Matrices Molecular Characterization, Total Research & Technology, Gonfreville 76700 Harfleur, France; orcid.org/0000-0003-1302-2850

Complete contact information is available at:

<https://pubs.acs.org/10.1021/acs.energyfuels.2c00486>

Funding

Part of this work was supported by NSF Division of Chemistry and Division of Materials Research through DMR-1644779 and the State of Florida

Notes

The authors declare no competing financial interest.

ACKNOWLEDGMENTS

Samples of Athabasca asphaltenes after catalytic hydroconversion were kindly provided by Dr Harvey Yarranton, University of Calgary.

ABBREVIATIONS USED

FT-ICR MS, Fourier-transform ion-cyclotron resonance mass spectrometry; IRMPD, infrared multiphoton dissociation; VPO, vapor pressure osmometry

REFERENCES

- (1) Strausz, O. P. Structural studies on resids: Correlation between structure and activity. In *Fundamentals of Resid Upgrading*, Heck, R. H., Degnan, T. F., Eds.; AIChE: New York, 1989; Vol. AIChE Symp. Ser. 273.
- (2) Liao, Z. W.; Zhao, J.; Creux, P.; Yang, C. P. Discussion on the structural features of asphaltene molecules. *Energy Fuels* **2009**, *23*, 6272–6274.
- (3) Karimi, A.; Qian, K.; Olmstead, W. N.; Freund, H.; Yung, C.; Gray, M. R. Quantitative evidence for bridged structures in asphaltenes by thin film pyrolysis. *Energy Fuels* **2011**, *25*, 3581–3589.
- (4) Rueda-Velasquez, R. I.; Freund, H.; Qian, K. N.; Olmstead, W. N.; Gray, M. R. Characterization of asphaltene building blocks by cracking under favorable hydrogenation conditions. *Energy Fuels* **2013**, *27*, 1817–1829.
- (5) Calemme, V.; Rausa, R. Thermal decomposition behavior and structural characteristics of asphaltenes. *J. Anal. Appl. Pyrolysis* **1997**, *40–41*, 569–584.
- (6) Ballard, D. A.; Chacón-Patiño, M. L.; Qiao, P.; Roberts, K. J.; Rae, R.; Dowding, P. J.; Xu, Z.; Harbottle, D. *Molecular Characterization of Strongly and Weakly Interfacially Active Asphaltenes by High-Resolution Mass Spectrometry*. **2020**, *34*, 13966–1397.
- (7) Chacón-Patiño, M. L.; Gray, M. R.; Niles, S. F.; Glatte, T.; Moulain, R.; Putman, J.; Smith, D. F.; McKenna, A. M.; Weisbord, C. W.; Giusti, P.; et al. Lessons Learned from a Decade-Long Assessment of Asphaltenes By Ultra-High-Resolution Mass Spectrometry and Implications for Complex Mixture Analysis. *Energy Fuels* **2021**, *35*, 16335–16376.
- (8) Nyadong, L.; Lai, J. F.; Thompsen, C.; LaFrancois, C. J.; Cai, X. H.; Song, C. X.; Wang, J. M.; Wang, W. High-Field Orbitrap Mass

Spectrometry and Tandem Mass Spectrometry for Molecular Characterization of Asphaltenes. *Energy Fuels* **2018**, *32* (1), 294–305.

(9) Dong, X.; Zhang, Y.; Milton, J.; Yerabolu, R.; Easterling, L.; Kenttamaa, H. I. Investigation of the relative abundances of single-core and multicore compounds in asphaltenes by using high-resolution in-source collision-activated dissociation and medium-energy collision-activated dissociation mass spectrometry with statistical considerations. *Fuel* **2019**, *246*, 126–132.

(10) Chacón-Patiño, M. L.; Rowland, S. M.; Rodgers, R. P. Advances in Asphaltene Petroleomics. Part 3. Dominance of Island or Archipelago Structural Motif Is Sample Dependent. *Energy Fuels* **2018**, *32*, 9106–9120.

(11) Neumann, A.; Chacón-Patiño, M. L.; Rodgers, R. P.; Rüger, C. P.; Zimmermann, R. Investigation of island/ single core and archipelago/ multicore enriched asphaltenes and their solubility fractions by thermal analysis coupled to high resolution Fourier-transform ion cyclotron resonance mass spectrometry. *Energy Fuels* **2021**, *35*, 3808–3824.

(12) Speight, J. G. *The Chemistry and Technology of Petroleum*, 4th ed.; CRC Press: Boca Raton, FL, 2006.

(13) Ancheyta, J.; Rana, M. S.; Furimsky, E. Hydroprocessing of heavy petroleum feeds: Tutorial. *Catal. Today* **2005**, *109* (1–4), 3–15.

(14) Wiehe, I. A. *Process Chemistry of Petroleum Macromolecules*; CRC Press: Boca Raton, FL, 2008; Vol. 121, p 427.

(15) Ovalles, C.; Rogel, E.; Lopez, J.; Pradhan, A.; Moir, M. Predicting Reactivity of Feedstocks to Resid Hydroprocessing Using Asphaltene Characteristics. *Energy Fuels* **2013**, *27* (11), 6552–6559.

(16) Klein, M. T.; Hou, G.; Bertolacini, R.; Broadbelt, L. J.; Kumar, A. *Molecular Modeling in Heavy Hydrocarbon Conversions*; CRC Press: Boca Raton, FL, 2005; p 262.

(17) Neurock, M.; Libanati, C.; Klein, M. T. Modelling of asphaltene reaction pathways: intrinsic chemistry. *Fundamentals of Resid Upgrading*; AIChE: New York, 1989; Vol. 85, pp 7–14.

(18) Neurock, M.; Libanati, C.; Nigam, A.; Klein, M. T. Monte carlo simulation of complex reaction systems: molecular structure and reactivity in modelling heavy oils. *Chem. Eng. Sci.* **1990**, *45* (8), 2083–2088.

(19) Jaffe, S. B.; Freund, H.; Olmstead, W. N. Extension of structure-oriented lumping to vacuum residua. *Ind. Eng. Chem. Res.* **2005**, *44* (26), 9840–9852.

(20) Trejo, F.; Ancheyta, J.; Morgan, T. J.; Herod, A. A.; Kandiyoti, R. Characterization of asphaltenes from hydrotreated products by SEC, LDMS, MALDI, NMR, and XRD. *Energy Fuels* **2007**, *21* (4), 2121–2128.

(21) Nagaishi, H.; Chan, E. W.; Sanford, E. C.; Gray, M. R. Kinetics of high-conversion hydrocracking of bitumen. *Energy Fuels* **1997**, *11*, 402–410.

(22) Wiehe, I. A. A phase separation kinetic model for coke formation. *Ind. Eng. Chem. Res.* **1993**, *32*, 2447–2457.

(23) Gray, M. R.; McCaffrey, W. C. Role of chain reactions and olefin formation in cracking, hydroconversion and coking of petroleum and bitumen fractions. *Energy Fuels* **2002**, *16*, 756–766.

(24) Alshareef, A. H.; Scherer, A.; Tan, X.; Azyat, K.; Stryker, J. M.; Tykwinski, R.; Gray, M. R. Formation of archipelago structures during thermal cracking implicates a chemical mechanism for the formation of petroleum asphaltenes. *Energy Fuels* **2011**, *25*, 2130–2136.

(25) Habib, F.; Diner, C.; Stryker, J. M.; Semagina, N.; Gray, M. R. Suppression of addition reactions during thermal cracking using hydrogen and sulfide catalyst. *Energy Fuels* **2013**, *27*, 6637–6645.

(26) Gray, M. R.; Le, T.; McCaffrey, W. C.; Berruti, F.; Soundararajan, S.; Chan, E.; Huq, I.; Thorne, C. Coupling of mass transfer and reaction in coking of thin films of Athabasca vacuum residue. *Ind. Eng. Chem. Res.* **2001**, *40*, 3317–3324.

(27) Behar, F.; Pelet, R. Characterization of asphaltenes by pyrolysis and chromatography. *J. Anal. Appl. Pyrolysis* **1984**, *7*, 121–135.

(28) Rahmani, S.; McCaffrey, W. C.; Dettman, H. D.; Gray, M. R. Coking kinetics of asphaltenes as a function of chemical structure. *Energy Fuels* **2003**, *17*, 1048–1056.

- (29) Saxena, A.; Diaz-Goano, C.; Dettman, H. Coking behavior during visbreaking. *J. Can. Petrol. Technol.* **2012**, *51*, 457–463.
- (30) Guitian, J.; Souto, A.; Ramirez, R.; Marzin, R.; Solari, B. Commercial design of a new upgrading process, HDH. In *Proc. Int. Symp. on Heavy Oil and Residue Upgrading and Utilization*; Han, C., Hsi, C., Eds.; International Academic, Beijing: Beijing, China, 1992; pp 237–247.
- (31) Chacón-Patiño, M. L.; Vesga-Martínez, S. J.; Blanco-Tirado, C.; Orrego-Ruiz, J. A.; Gómez-Escudero, A.; Combariza, M. Y. Exploring Occluded Compounds and Their Interactions with Asphaltene Networks Using High-Resolution Mass Spectrometry. *Energy Fuels* **2016**, *30*, 4550–4561.
- (32) Smith, D. F.; Podgorski, D. C.; Rodgers, R. P.; Blakney, G. T.; Hendrickson, C. L. 21 T FT-ICR Mass Spectrometer for Ultrahigh-Resolution Analysis of Complex Organic Mixtures. *Anal. Chem.* **2018**, *90* (3), 2041–2047.
- (33) Chacón-Patiño, M. L.; Rowland, S. M.; Rodgers, R. P. *The Compositional and Structural Continuum of Petroleum from Light Distillates to Asphaltenes: The Boduszynski Continuum Theory As Revealed by FT-ICR Mass Spectrometry*; American Chemical Society: Washington, DC, 2018; Vol. 1282, pp 113–171.
- (34) Niles, S. F.; Chacón-Patiño, M. L.; Smith, D. F.; Rodgers, R. P.; Marshall, A. G. Comprehensive Compositional and Structural Comparison of Coal and Petroleum Asphaltenes Based on Extrography Fractionation Coupled with Fourier Transform Ion Cyclotron Resonance MS and MS/MS Analysis. *Energy Fuels* **2020**, *34* (2), 1492–1505.
- (35) Chacón-Patiño, M. L.; Rowland, S. M.; Rodgers, R. P. Advances in asphaltene petroleomics. Part 1: Asphaltenes are composed of abundant island and archipelago structural motifs. *Energy Fuels* **2017**, *31*, 13509–13518.
- (36) Chacón-Patiño, M. L.; Rowland, S. M.; Rodgers, R. P. Advances in Asphaltene Petroleomics. Part 2: Selective Separation Method That Reveals Fractions Enriched in Island and Archipelago Structural Motifs by Mass Spectrometry. *Energy Fuels* **2018**, *32*, 314–328.
- (37) Juyal, P.; McKenna, A. M.; Fan, T. G.; Cao, T.; Rueda-Velasquez, R. L.; Fitzsimmons, J. E.; Yen, A.; Rodgers, R. P.; Wang, J. X.; Buckley, J. S.; et al. Joint Industrial Case Study for Asphaltene Deposition. *Energy Fuels* **2013**, *27* (4), 1899–1908.
- (38) Siskin, M.; Kelemen, S. R.; Eppig, C. P.; Brown, L. D.; Afeworki, M. Asphaltene chemical structure and chemical influences on the morphology of coke produced in delayed coking. *Energy Fuels* **2006**, *20*, 1227–1234.
- (39) Sheremata, J. M.; Gray, M. R.; Dettman, H. D.; McCaffrey, W. C. Quantitative molecular representation and sequential optimization of Athabasca asphaltenes. *Energy Fuels* **2004**, *18*, 1377–1384.
- (40) Boduszynski, M. M. Composition of heavy petroleums. 2. Molecular characterization. *Energy Fuels* **1988**, *2*, 597–613.
- (41) Carrillo, J. A.; Corredor, L. M.; Valero, M. L. Visbreaking of the heavy crude oils: Castilla, Rubiales and Nare-Jazmin. *Prepr. Pap. Am. Chem. Soc., Div. Fuel Chem.* **2004**, *49* (2), 496.
- (42) Powers, D. P.; Sadeghi, H.; Yarranton, H. W.; van den Berg, F. G. A. Regular solution based approach to modeling asphaltene precipitation from native and reacted oils: Part I, molecular weight, density, and solubility parameter distributions of asphaltenes. *Fuel* **2016**, *178*, 218–233.
- (43) Gray, M. R.; Yarranton, H. W.; Chacón-Patiño, M. L.; Rodgers, R. P.; Bouyssiére, B.; Giusti, P. Distributed Properties of Asphaltene Nanoaggregates in Crude Oils: A Review. *Energy Fuels* **2021**, *35*, 18078–18103.
- (44) Acevedo, N.; Mouliau, R.; Chacón-Patiño, M. L.; Mejia, A.; Radji, S.; Daridon, J.-L.; Barrère-Mangote, C.; Giusti, P.; Rodgers, R. P.; Piscitelli, V.; et al. Understanding Asphaltene Fraction Behavior through Combined Quartz Crystal Resonator Sensor, FT-ICR MS, GPC ICP HR-MS, and AFM Characterization. Part I: Extrography Fractionations. *Energy Fuels* **2020**, *34* (11), 13903–13915.
- (45) Hsu, C. S.; Lobodin, V. V.; Rodgers, R. P.; McKenna, A. M.; Marshall, A. G. Compositional Boundaries for Fossil Hydrocarbons. *Energy Fuels* **2011**, *25*, 2174–2178.
- (46) Purcell, J. M.; Merdrignac, I.; Rodgers, R. P.; Marshall, A. G.; Gauthier, T.; Guibard, I. Stepwise Structural Characterization of Asphaltenes during Deep Hydroconversion Processes Determined by Atmospheric Pressure Photoionization (APPI) Fourier Transform Ion Cyclotron Resonance (FT-ICR) Mass Spectrometry. *Energy Fuels* **2010**, *24* (4), 2257–2265.
- (47) Podgorski, D. C.; Corilo, Y. E.; Nyadong, L.; Lobodin, V. V.; Bythell, B. J.; Robbins, W. K.; McKenna, A. M.; Marshall, A. G.; Rodgers, R. P. Heavy petroleum composition. 5. Compositional and structural continuum of petroleum revealed. *Energy Fuels* **2013**, *27* (3), 1268–1276.
- (48) Ruiz-Morales, Y. HOMO-LUMO Gap as an Index of Molecular Size and Structure for Polycyclic Aromatic Hydrocarbons (PAHs) and Asphaltenes: A Theoretical Study. *J. Phys. Chem. A* **2002**, *106* (46), 11283–11308.
- (49) Yuan, G.; Xue, Z.; Cui, Z.; Westwood, A.; Dong, Z.; Cong, Y.; Zhang, J.; Zhu, H.; Li, X. Constructing the Bridge from Isotropic to Anisotropic Pitches for Preparing Pitch-Based Carbon Fibers with Tunable Structures and Properties. *ACS Omega* **2020**, *5* (34), 21948–21960.
- (50) Mochida, I.; Zhao, X. Z.; Sakanishi, K.; Yamamoto, S.; Takashima, H.; Uemura, S. Structure and properties of sludges produced in the catalytic hydrocracking of vacuum residue. *Ind. Eng. Chem. Res.* **1989**, *28*, 418–421.
- (51) Panariti, N.; Del Bianco, A.; Del Piero, G.; Marchionna, M.; Carniti, P. Petroleum residue upgrading with dispersed metal catalysts. Part 2. Effect of operating conditions. *Appl. Catal., A* **2000**, *204*, 215–222.